



DOI: 10.34910/MCE.101.7

## Basalt fiber reinforced expanded clay concrete for building structures

V.V. Galishnikova, M. Kharun, D.D. Koroteev, P.C. Chiadighikaobi\*

Peoples Friendship University of Russia (RUDN University), Moscow, Russian Federation

\* E-mail: [passydking2@mail.ru](mailto:passydking2@mail.ru)

**Keywords:** expanded clay concrete, basalt fiber, compressive strength, flexural strength, finite element analysis

**Abstract.** Expanded clay concrete is a perspective structural material because of its lightweight, heat and sound insulating properties. However, due to its brittleness and low strength to flexure and compression it cannot be used in load bearing structures. Adding basalt fiber in concrete increases mechanical properties. The research work presents an experimental study of the mechanical behavior of structural expanded clay basalt fiber concrete. The main purpose of this study was to test the effect of chopped basalt fiber in expanded clay concrete to improve its strength. An experimental characterization of mechanical behavior by compressive and flexural tests was achieved. Dispersed chopped basalt fiber was used as reinforcement of specimens with sizes of 100×100×100 mm and 100×100×400 mm. Mathematical models for determining the compressive strength and the flexural strength of the expanded clay concrete depending on the proportion of basalt fiber and the curing period are developed. The finite element analysis was done by using ANSYS software, a model was developed to validate the different results obtained experimentally. The experimental results show that high percent of basalt fiber in the expanded clay concrete gives higher strength. In effect, an influence directly on the failure mode was observed on expanded clay concrete without basalt fiber and then read by the value of strength and ultimate deformation.

### 1. Introduction

For many years now, it has become very important in construction for rehabilitation and strengthening of reinforced concrete. Reinforced concrete structure as the whole element can withstand tensile flexural loading, however, the concrete cover layer in such structure is not reinforced and cannot withstand such loading, it causes cracking of the structures during their operation which leads to corrosion of steel reinforcement and damage of the structure [1–3]. The reinforcement materials for concrete structures varies based on the properties. With the air pollution related problems increasing globally and rising of the mean temperature around the globe, it became a necessity investigate to investigate new solutions in order to diminish the magnitude of such environmental issues [4]. The author investigated the use of bamboo in concrete reinforcement to serve in high temperate region and solve environmental issues.

The tensile flexural strength of concrete is an important method to determine cracking behavior of concrete and to compute deflection under flexure. Many factors have been shown to influence on the flexural tensile strength, particularly the level of concrete strength, size of member, age of concrete and confinement to flexure member etc [5].

The physical, mechanical and durability properties of basalt fiber (BF) reinforced lightweight pumice concrete including water absorption, bulk density, strength and sulfate attack resistance were investigated [5, 6]. In the study [6], Taguchi method was proposed by the author to optimize compressive strength, flexural strength and sulfate resistance properties.

Recently, basalt fiber reinforced polymer (BFRP) has been developed because of its properties, such as high elastic modulus and elastic strength, better tensile strength than E-glass fibers, better failure strain than carbon fibers [7–10]. In addition, it has good resistance to chemical attack and high temperature, impact load and fire with less poisonous fumes, lower cost as compared with other types of fibers [11–13]. BF can be



considered as a green product as compared with other materials because the natural raw materials are used for their production, any chemical additives or hazardous materials are not used in the melting process, any chemical does not appear during the production process, which is dangerous to health [14–16].

The use of fiber reinforced polymer (FRP) materials in flexural strengthening of reinforced concrete shallow beams has been investigated quite extensively by many researchers [17–20]. The results of these investigations have demonstrated the effectiveness of different forms of FRP systems to achieve the desired effects.

In most part of research works [21–25], the authors pointed that concrete, reinforced with BF, has high flexural strength and tensile strength as compared with concrete without the fiber. However, compressive strength of concrete with BF increases slightly at the early age and even decreases at the late age.

Generally, there is less information documented on the workability of expanded clay as an aggregate in concrete, reinforced with BF [26]. From our point of view, expanded clay concrete (ECC) is a perspective structural material because of its certain advantages, such as lightweight, heat and sound insulating properties [27–33]. However, due to its brittleness and low strength to flexure and compression it cannot be used in load bearing structures. Safe performance of connecting joint applied to different concrete ages is highly important

when joints are placed in composite structures since joint is involved in mutual deformation of precast and monolithic concretes [34].

In research work [35], the authors considered the energy efficiency light-weight wall technology for over story of buildings. Further in the research work was developed a mathematical model of non-stationary heat transfer through the enclosing wall using the lightweight wall technology and evaluated the efficiency of various designs of lightweight wall.

The introduction of silica fume into the cement system lowers the pH of the aqueous extract by 28 days of hardening relative to the composition without silica fume by 3 %, which indicates a decrease in the CaO content in the system and better preservation of basalt fiber. It confirmed by the absence of changes in the pH of aqueous extracts of compositions with fiber and without fiber in compositions containing MK-85 for all periods of hardening of cement stone. Thus, to increase the durability of basalt fiber in cement systems effectively use silica fume (micro silica) addition, which reduces the amount of free lime in the environment of hydrating cement [36]. Series of studies and experiments on the durability of basalt fiber reinforced concrete, the construction environments and methods of constructions are explained in detail [37].

Finite element analysis is a numerical method for analyzing complex structural problems. Like homogeneous materials, composite materials can also be analyzed using pre- and post-processing facilities of ANSYS to study their behavior under different load conditions [38], temperature distribution over the thickness of the experimental wall cover can also be analyzed in ANSYS [39].

The displacements of the concrete structures are small compared to the dimensions of the structure and hence in the present study geometric non-linearity is neglected. Since the concrete is a non-homogeneous material and behaves linearly over a small percentage of its strength, material non-linearity is considered [40].

Nonlinear finite element analysis is a powerful tool in determining the internal stress, strain distribution in concrete structures. Nonlinear analysis gives enhanced data of serviceability and ultimate strength. The finite element analysis is adopted with the different material nonlinearities such as stress-strain behavior of concrete, cracking of concrete [41].

Taking the above into account, the aim of this research work is to study the influence of chopped basalt fiber on physical-mechanical properties of ECC, especially compressive and flexural behavior of the concrete.

The following tasks are determined to reach the above aim:

- Preparation and test of ECC specimens, reinforced with and without dispersed chopped BF, with sizes of 100×100×100 mm and 100×100×400 mm;
- Determination of compressive and flexural strength of ECC specimens with and without BF;
- Finite element analysis of compressive and flexural behaviors of the ECC structures with BF by modeling nonfinite element solutions (data), derived from laboratory experiments in a finite element software (ANSYS) and inputting the boundary conditions for better results.

Due to the properties of ECC reinforced with dispersed BF, this concrete can be used in high temperature regions.

This research paper investigates and analyses the strength of ECC reinforced with dispersed BF. Due to the brittleness of ECC mostly in flexure, this paper is faced with the task to investigate, identify and suggest the material for reinforcement that will cure the brittleness, increase the strength of ECC.

## 2. Materials and methods of research

According to the plan of study the following materials were used to prepare ECC specimens for determination of compressive strength and flexural strength:

- Lightweight Expanded Clay Aggregate (LECA) with fractions of 5-10 mm = 200 kg/m<sup>3</sup> as the coarse aggregate;
- Quartz sand with fineness modulus of 2.7 = 585 kg/m<sup>3</sup> as the fine aggregate;
- Quartz flour of 50 µm = 100 kg/m<sup>3</sup> as the mineral filler;
- Portland cement CEM I 42.5 N = 500 kg/m<sup>3</sup> as the binder;
- Micro silica = 62.5 kg/m<sup>3</sup> and fly ash = 62.5 kg/m<sup>3</sup> as the organo-mineral additives;
- SikaPlast®Concrete in liquid form = 8 l/m<sup>3</sup> as the super plasticizing and water reducing admixture;
- Tap water = 255 l/m<sup>3</sup> for mixing.

LECA used in this experimental study was obtained from the Production Plant "Keramzit", Serpukhov District in Moscow Region, Russia. The physical properties and sieve analysis of LECA used in this study is illustrated in Table 1.

**Table 1. Physical properties and sieve analysis of LECA.**

Physical Property	Value
Specific gravity	0.69
Fineness modulus	5.93
Bulk density (compacted), [kg/m <sup>3</sup> ]	278
Water absorption (24 h), [%]	26.4
Sieve Analysis, [mm]	Cumulative Percent by weight passing
10.0	90.4
8.0	5.7
5.0	3.9
3.0	0

Before adding LECA to concrete mix, the coarse aggregate was pre-immersed in the water for 24 hours before mixing. The LECA is removed from the water and placed on a sieve for 2 hours to dry off the water in order to reach to almost saturated surface dry condition.

Quartz sand and quartz flour used in the experiment were obtained from the Quarry Plant "Tyutchevo", Naro-Fominsky District in Moscow Region, Russia. The binder Portland cement CEM I 42.5 N, mineral additives micro silica and fly ash were obtained from the Maltsovsky Cement Plant, Fokino District, Bryansk Region, Russia.

The physical properties of quartz sand and the chemical compositions of quartz flour, Portland cement, micro silica and fly ash respectively are presented in Tables 2 and 3.

**Table 2. Physical properties of quartz sand.**

Physical Property	Value
Grain size, [mm]	0.5–1.0
Bulk density (compacted), [kg/m <sup>3</sup> ]	1430
Hardness (on the Mohs scale)	7
Crushability	0.3
Humidity, [%]	1.7

**Table 3. Chemical compositions of quartz flour, Portland cement, micro silica and fly ash in percentage (%).**

Chemical Elements	SiO <sub>2</sub>	Al <sub>2</sub> O <sub>3</sub>	Fe <sub>2</sub> O <sub>3</sub>	K <sub>2</sub> O	CaO	MgO	SO <sub>3</sub>	P <sub>2</sub> O <sub>5</sub>	TiO	MnO	Na <sub>2</sub> O
Quartz Flour	99.63	0.23	0.12	-	0.02	-	-	-	-	-	-
Portland Cement	21.90	4.86	3.3	0.56	65.77	1.15	2.1	-	-	-	0.36
Micro silica	98.77	0.23	0.07	0.26	0.31	0.04	0.17	-	-	-	0.15
Fly Ash	66.24	19.81	6.41	1.39	3.13	1.21	-	0.36	0.86	0.05	0.54

SikaPlast® Concrete is the super plasticizing and water reducing admixture used in this experiment and it is a brown color aqueous solution of modified polycarboxylate esters and lignosulfonates.

The chopped BF, used in this study, was obtained from a famous BF Manufacturing Plant known as Russkiy Bazalt, located in Chelyabinsk, Russia. Table 4 below presents the chemical compositions of chopped BF used in this experiment.

**Table 4. Chemical compositions of chopped BF.**

Chemical Elements	SiO <sub>2</sub>	Al <sub>2</sub> O <sub>3</sub>	FeO + Fe <sub>2</sub> O <sub>3</sub>	Na <sub>2</sub> O + K <sub>2</sub> O	CaO	MgO	TiO <sub>2</sub>	Others
Percentage (%)	57.3	15.4	11.7	1.9	7.3	4.1	1.6	0.7

Five different mixes of ECC were accepted for this study, containing of the above mixes and the chopped BF with diameter of 15 µm and length of 20 mm in the ratio of 1:0, 1:0.045, 1:0.09, 1:0.012 and 1:0.016 by weight.

Experimental study of ECC was carried out in accordance with the CIS Interstate Standard GOST 10180-2012 [42], considering the requirements of ACI 211.1-91 [43].

Total 10 series of ECC test specimens were produced from the stated compositions with dimensions of 100×100×100 mm in 5 series; 100×100×400 mm in 5 series.

In accordance with the plan of experiment, each series consists of 9 specimens, total 90 specimens. All ECC specimens were cured in air-humid condition in wet sawdust at the room temperature of 19–22 °C.

Experimental study of ECC was carried out at the curing periods of 7, 14 and 28 days on a hydraulic press of up to 1500 kN at the compression test, and up to 150 kN at the flexural test.

The destruction of the surface of the fiber occurs when its interaction with hydrated lime released during the hardening process. In order to increase fiber resistance, silica fume was additionally introduced into the composition of cement concrete. Detailed research on this is seen in the study [36].

Mathematical processing of the experimental data was carried out based on probability theory and mathematical statistics which allowed obtaining the results of experimental study with the reliability of  $\alpha \approx 0.95$ .

Using of the mentioned materials to produce ECC specimens, and their study by the above method allowed obtaining the statistically significant results of experimental study.

For finite element analysis ANSYS software was chosen. It is a finite element general-purpose modeling package for solving numerical and wide range of mechanical problems. These problems can be solved using static linear structural analysis [41].

In general, a finite element analysis and solution in ANSYS may be broken into three stages. Before these three stages are listed, the project must be specialized. For the project analyzed in this research paper, structural was selected in the preferences. The three main stages are:

1. Preprocessing – defining the problem: it is necessary that every task and problem be defined. The major steps in preprocessing are:

- a. Define key points/lines/areas/volumes;
- b. Define element type and material/geometric properties;
- c. Mesh lines/areas/volumes as required.

2. Solution – assigning loads, constraints, and solving it is necessary to specify the loads (pressure) and constraints then, solve the resulting set of equations.
3. Postprocessing – further processing and viewing of the results are:
  - a. Lists of nodal displacements;
  - b. Element forces and moments;
  - c. deflection plots;
  - d. Stress contour diagrams or temperature maps. But in this research, the displacement at all degrees of freedom was checked [38].

To calculate tasks in ANSYS software, the finite element method is used. The essence of this method is that the continuous medium is replaced by a finite number of structural elements of finite size, connected with each other only at the nodal points.

To analyze the concrete, some important properties and conditions must be considered. These properties are modules of elasticity and Poisson's ration which were derived from the laboratory experiments of the ECC with BF. For comprehensive strength, a load of 22.5 MPa was imposed on the analysis in Fig. 6, 28.5 MPa in Fig. 7 and 36.2 MPa in Fig. 8. The dimensions of ECC with BF specimen are 100×100×100 mm.

For flexural strength, a load of 3.7 MPa was imposed on the analysis of Fig. 9, 4.9 MPa in Fig. 10, 6.5 MPa in Fig. 11 [39]. The dimensions of the ECC specimen are 6000×6000×150 mm. A boundary condition of all degrees of freedom (UX, UY, UZ) = 0 for the support was considered making the support fixed. One of the most important stage in finite element analysis in ANSYS software is the element type and property (Fig. 1). In modeling and analyzing this concrete cube and prisms, brick 8 node 185 element property is used.

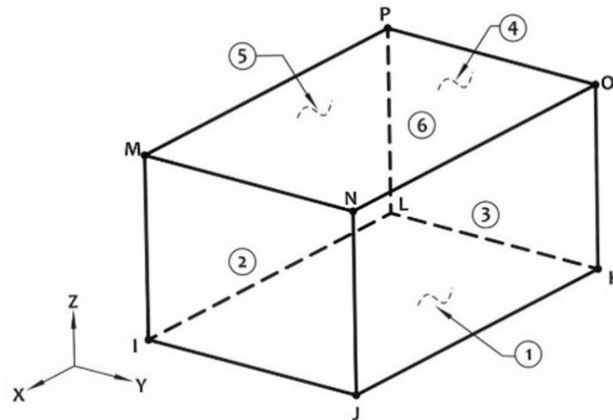


**Figure 1. Solid 185 homogeneous structural solid.**

Fig. 1 expresses the element type used. Where letters I-P show the nodes and numbers 1-6 show the solid plane (surface) of the concrete solid [40].

Brick 8 node 18 means SOLID 185. It is a 3D element consisting 8 nodes in it. SOLID 185 is used for 3D modeling of solid structures. It is expressed by 8 nodes with 3 degrees of freedom at each node. This element type is assumed to possibly can undergo plasticity, stress stiffness, creep large deflection, and large strain.

### 3. Result and Discussion

The most important physical and mechanical properties of concrete are the compressive strength and the flexural strength. In the framework of this research the experimental determination of the compressive strength and the flexural strength of ECC produced with chopped BF and without BF were carried out. The experimental results are gotten at structural strength. The properties of basalt fiber like thermal resistance, acidic resistance, water resistance give this concrete a high durability which are fully illustrated by previous authors [36, 37].

Results of the laboratory tests of ECC specimens of 100×100×100 mm on the compressive strength are shown in Table 5.

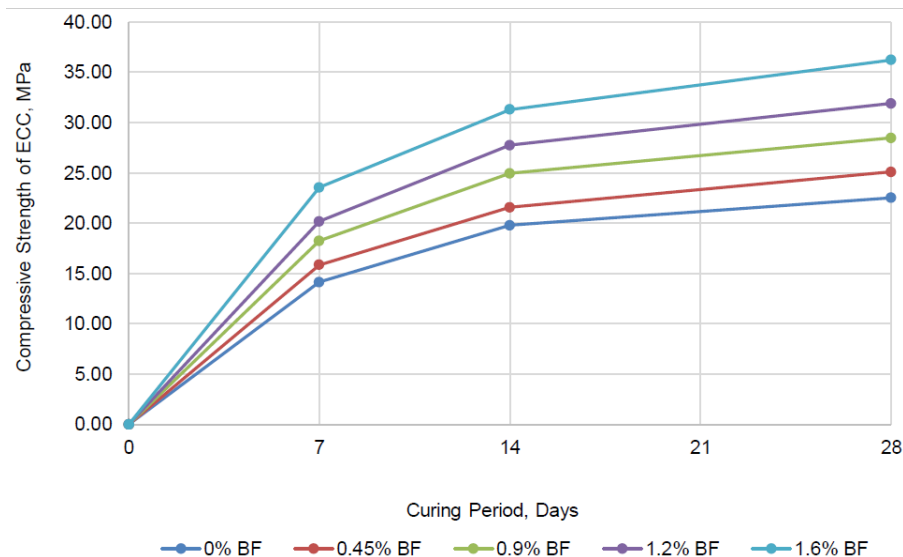
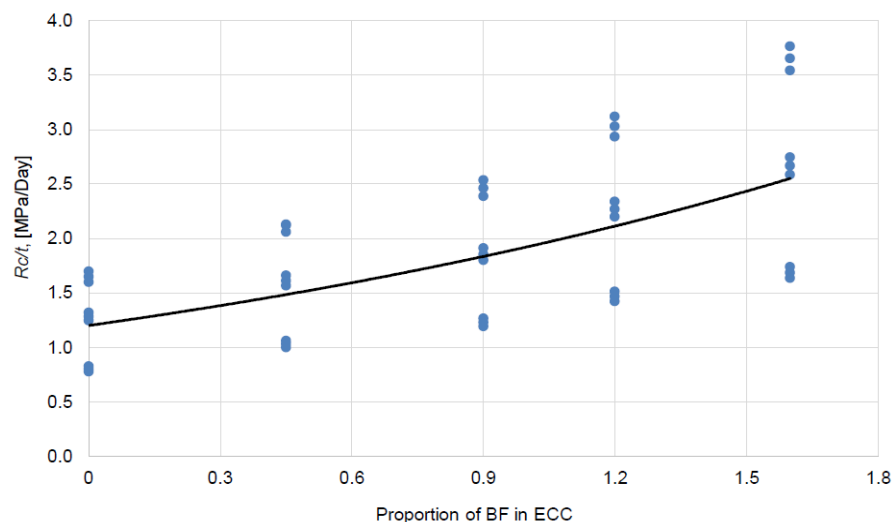
**Table 5. Results of the laboratory tests of ECC specimens of 100×100×100 mm on the compressive strength.**

Curing period, [days]	Compressive strength, [MPa]				
	0% BF	0.45% BF	0.9% BF	1.2% BF	1.6% BF
7	14.156	15.862	18.247	20.191	23.572
14	19.794	21.597	24.972	27.772	31.328
28	22.535	25.122	28.498	31.927	36.236

Fig. 2 shows the diagrams of changes in compressive strength of ECC depending on the curing period.

Experimental study of ECC specimens (Table 5 and Fig. 2) showed that addition of BF in ECC resulted an increase in the compressive strength which differs from some of the experimental studies done by previous authors where the authors checked the compressive strength of conventional high strength concrete with addition of chopped basalt fiber. Their results showed that addition of chopped basalt fiber in these conventional concrete specimens reduced the compressive strength of the concrete [17, 18, 19]. The results also showed that the compressive strength in 7 days of curing can reach about 60 % of the compressive strength of 28 days curing period regardless of whether ECC is without BF or with BF.

Fig. 3 shows the dependency of the compressive strength of ECC on the proportion of BF and the curing period.

**Figure 2. Compressive strength of ECC depending on the curing period of ECC specimens of 100×100×100 mm.****Figure 3. Dependency of the compressive strength of ECC on the percentage of BF and the curing period.**

Based on analytical data (Fig. 3), using the probability theory and mathematical statistics, a mathematical model of compressive strength of ECC depending on the percentage of cement and curing period was developed:

$$R_C = R_C^t + \frac{1.245 \times t \times e^{45 \times F}}{e^{45 \times F} + \frac{e^{45 \times F}}{t_F}} \quad (1)$$

where  $R_C$  is compressive strength of ECC, MPa;  $R_C^t$  is compressive strength of ECC (without BF) of the corresponding grade on the day of determination, MPa; 1.245 is coefficient of compressive strength changes of ECC with BF over the period, MPa/day;  $e$  is exponential function,  $e \approx 2.71828$ ;  $F$  is proportion of BF in ECC, in relative units;  $t$  is curing period, day ( $t \leq 28$  days);  $t_F$  – exposure of BF in ECC,  $t_F = t$  without unit.

The proposed mathematical model is advisable to apply for assessment of the compressive strength of ECC with the accuracy of  $\pm 4-5\%$  and the determination coefficient of  $R^2 = 0.935$ . It allows determining the permissible load on the structure that works on compression, such as walls.

Results of the laboratory tests of ECC specimens of 100×100×400 mm on the flexural strength are shown in Table 6.

**Table 6. Results of the laboratory tests of ECC specimens of 100×100×400 mm on the flexural strength.**

Concrete curing, [days]	Flexural strength, [MPa]				
	0% BF	0.45% BF	0.9% BF	1.2% BF	1.6% BF
7	2.422	2.844	3.219	3.728	4.397
14	3.298	3.836	4.411	5.028	5.855
28	3.658	4.278	4.905	5.668	6.488

Fig. 4 shows the diagrams of changes in flexural strength of ECC depending on the curing period.

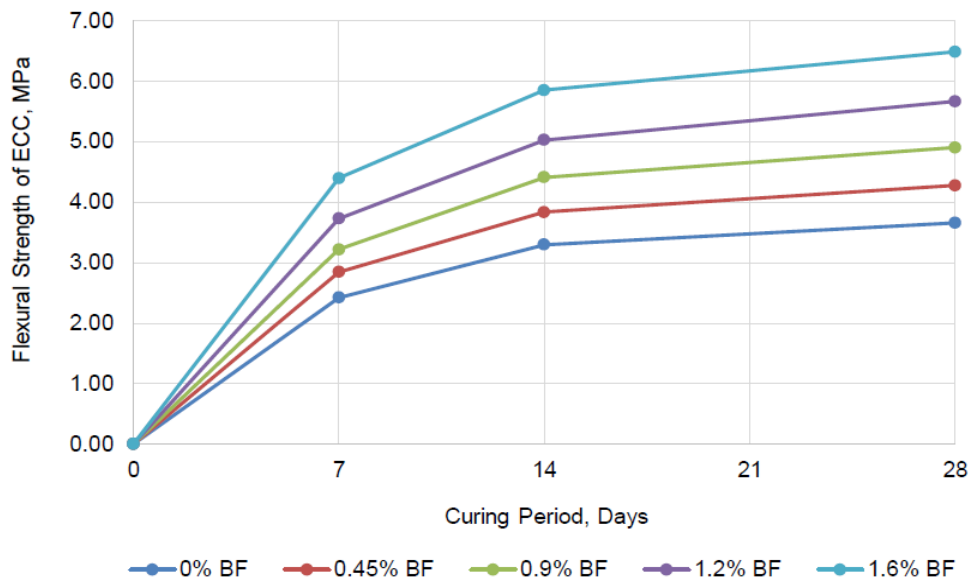


**Figure 4. Flexural strength of ECC depending on the curing period of ECC specimens of 100×100×400 mm.**

Analysis of the diagrams of the Fig. 2 and 4 shows that the strength growth in ECC specimens is smooth and uniform as in conventional concrete regardless of whether ECC is without BF or with BF. Though the growths in the flexural strength of concrete with addition of chopped basalt fiber were faster and higher in ECC than in conventional concrete, the growth in both types of concrete are significant in comparison with experiments of other researchers [17–20].

Analyzing the diagrams in Fig. 2 and 4, and tables 2 and 3, it can be concluded that ECC with 0.9 wt.% BF increases the compressive strength by more than 20 %, while 1.6 wt.% BF enhances more than 50 %, and the flexural strength by more than 30 %, while 1.6 wt.% BF enhances more than 75 %, i.e. a high percentage of BF in ECC gives a higher strength.

Fig. 5 shows the dependency of the flexural strength of ECC on the proportion of BF and the curing period.

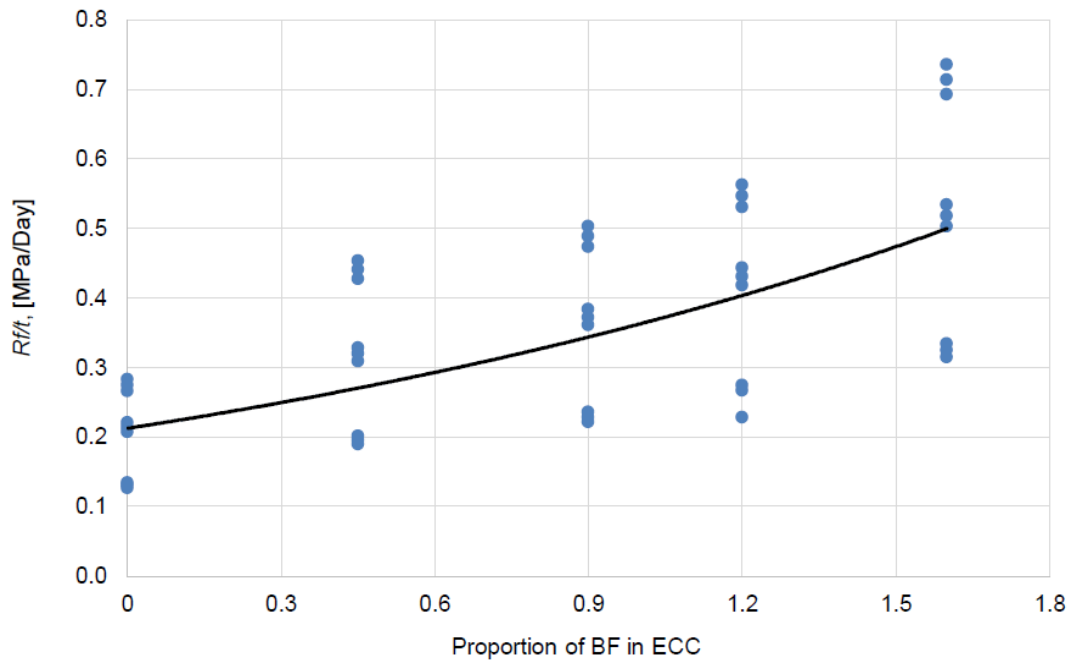


**Figure 5. Dependency of the flexural strength of ECC on the proportion of BF and the curing period.**

Analysis of diagrams in Fig. 3 and Fig. 5 shows that the nature of changes of compressive strength and flexural strength of ECC on the proportion of BF and the curing period is identical and grows exponentially.

Based on the analytical data (Fig. 5), using the probability theory and mathematical statistics, a mathematical model of flexural strength of ECC depending on the percentage of cement and curing period was developed:

$$R_f = R_f^t + \frac{0.215 \times t \times e^{53 \times F}}{e^{53 \times F} + \frac{e^{53 \times F}}{t_F}} \quad (2)$$

where  $R_f$  is flexural strength of ECC, MPa;  $R_f^t$  is flexural strength of ECC (without BF) of the corresponding grade on the day of determination, MPa; 0.215 is coefficient of flexural strength changes of ECC with BF over the period, MPa/day;  $e$  is exponential function,  $e \approx 2.71828$ ;  $F$  is proportion of BF in ECC, in relative units;  $t$  is curing period, day ( $t \leq 28$  days);  $t_F$  is exposure of BF in ECC,  $t_F = t$  without unit.

The proposed mathematical model is advisable to apply for forecasting the flexural strength of ECC with the accuracy of  $\pm 4$ -5% and the determination coefficient of  $R^2 = 0.927$ . It allows determining the permissible load on the structure that works on flexion, such as slabs.

From the non-finite element results derived from laboratory experimental results, the data was inputted in the ANSYS finite element software to derive the deformation effect and influence of the load imposed on the ECC with and without BF. The results derived from finite element analysis is illustrated in Fig. 6–11. In Fig. 6–11, the maximum displacements and maximum stress are denoted as DMX and SMX respectively.



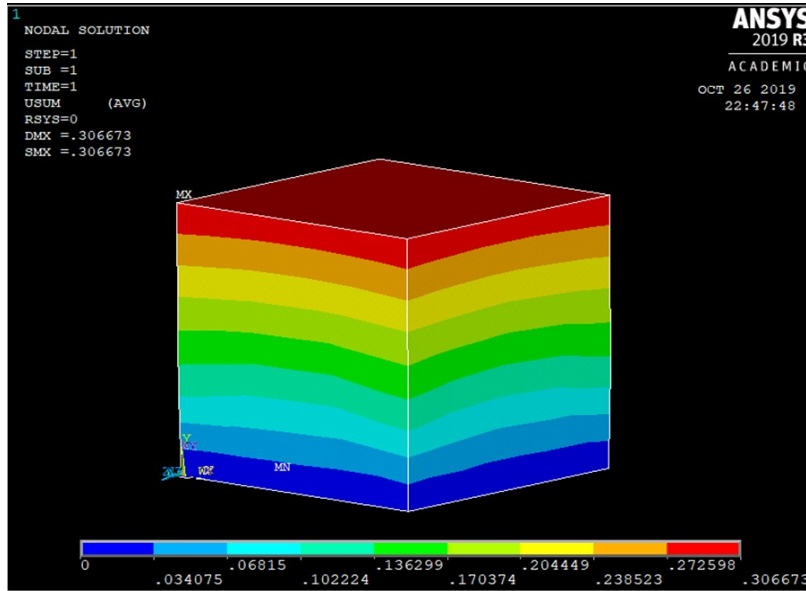


Figure 6. Nodal solution of ECC without BF.

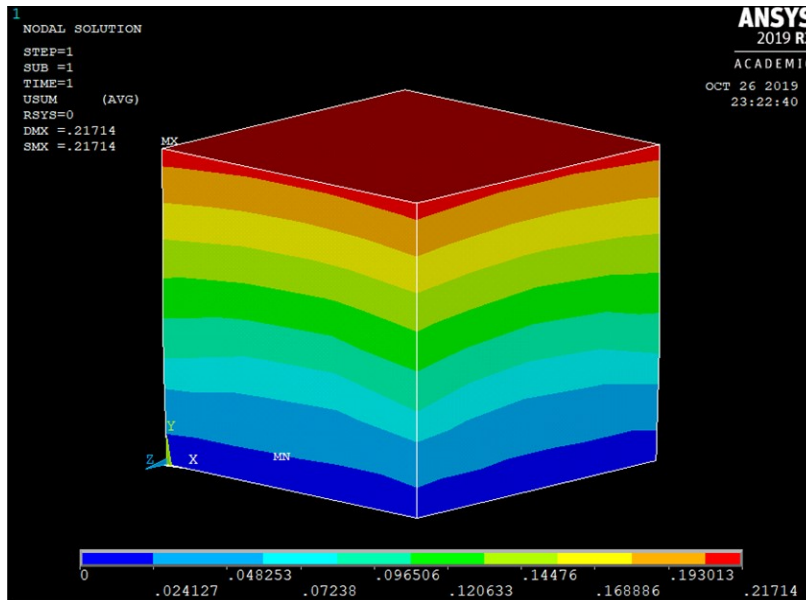


Figure 7. Nodal solution of ECC with 0.9 % BF.

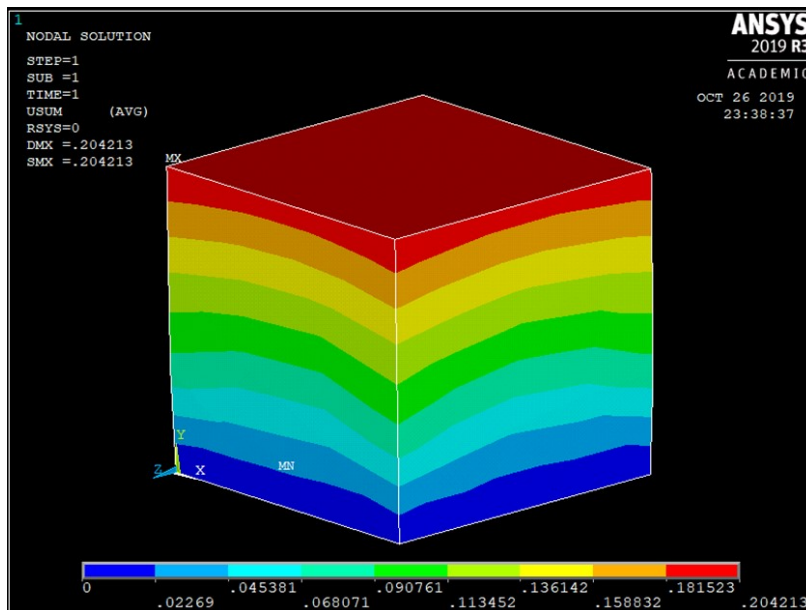


Figure 8. Nodal solution of ECC with 1.6 % BF.

The results derived from the finite element analysis, it is seen that ECC without BF (Fig. 6) shows more displacement when compared to the results of Fig. 7 and 8, while Fig. 6 shows more displacement than the result in Fig. 8.

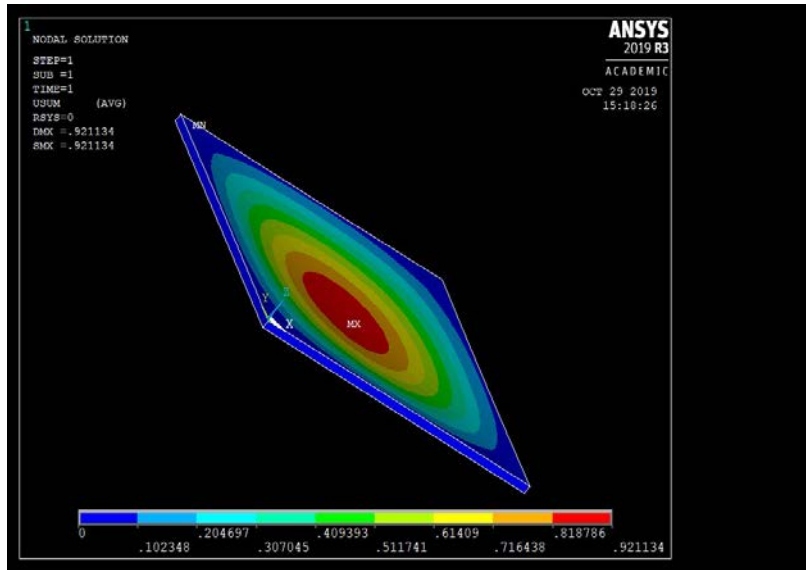


Figure 9. Nodal solution of ECC slab without BF.

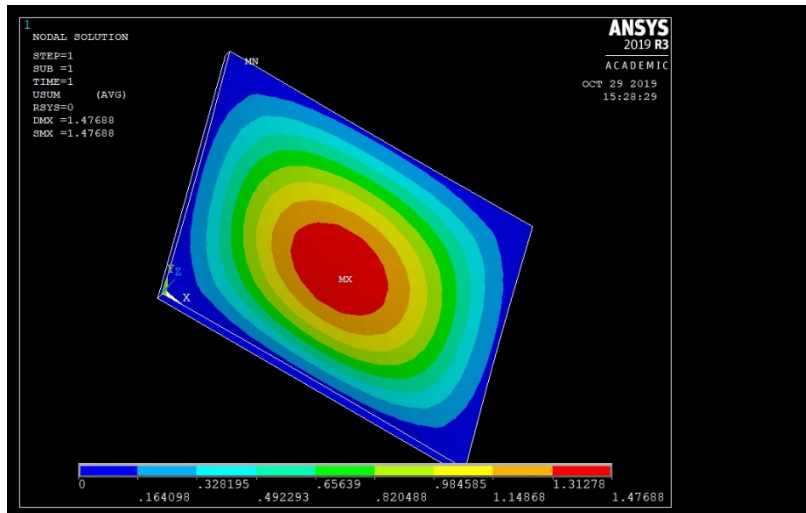


Figure 10. Nodal solution of ECC slab with 0.9 % BF.

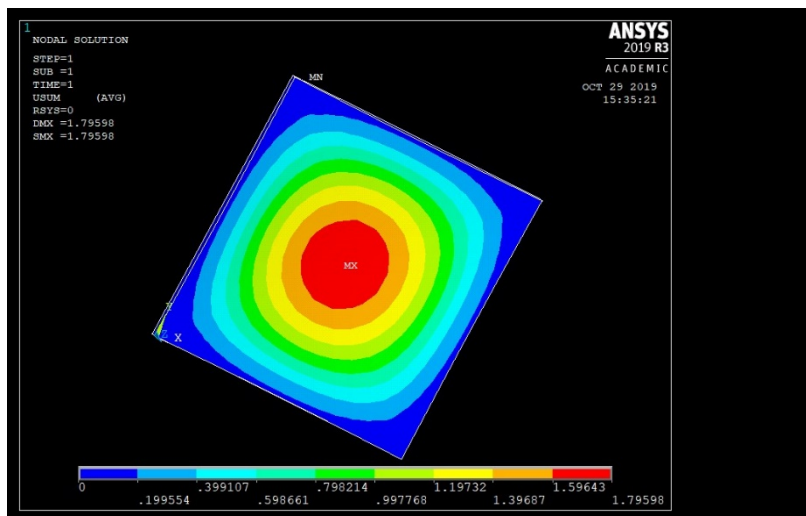


Figure 11. Nodal solution of ECC slab with 1.6 % BF.

The results from the ANSYS finite element analysis Fig. 6–11 show the maximum and minimum displacements at the critical stages. The results derived from the finite element analysis, it is seen that ECC

slab without BF (Fig. 9) shows more less displacement when compared to the results of Fig. 10 and 11, while Fig. 10 shows less displacement than the result in Fig. 11. Reason for this increase in displacement of the slab with increase in the percent of BF is, as a result, of the slab span. The boundary conditions for this analysis is all degrees of freedom where ( $U_x$ ,  $U_y$  and  $U_z$ ) = 0. The loads applied are the loads from the flexural strength on 28<sup>th</sup> day of Table 5.

From the experimental results, ECC with 1.6 % BF has highest compressive and flexural strength. To model ECC structures in a finite element software ANSYS, the dimensions and properties of this structure should be inputted in the software.

The finite element analysis using ANSYS software allowed to validate the different results obtained experimentally, such as for the specimens with 100×100×100 mm dimensions shows an increase of strength with increase of BF dosage, while in the specimens with 6000×6000×150 mm dimensions taken as slab shows a reduction in strength with increase in BF dosage that can be justified by supporting beams and columns at shorter distances.

#### 4. Conclusion

Based on the study, the following conclusion can be drawn:

1. BF works well with ECC, and high percentage of BF in ECC gives higher compressive and flexural strength which contradicts the experimental motions that addition of BF in concrete decreases the compressive strength of concrete. This is so because of the compatibility of ECC with BF. And confirms the research work done by previous authors reviewed in this study which showed that the quantity of fiber in concrete affects strength of concrete.

2. The proposed mathematical models allow to determine the permissible loads on the structures during construction works. From the finite element analysis using ANSYS software allows to validate the different results obtained experimentally.

3. Analysing the results of previous authors, BF showed better effects to the concrete if compared to steel fiber and glass fiber. Based on the review analysis, it is seen that there are very little or no information on the workability of ECC and BF, but this research experiment showed better results based on the properties of expanded clay aggregate and BF.

#### 5. Acknowledgements

The publication has been prepared with the support of the "RUDN University Program 5-100".

#### References

1. Francois, R., Laurens, S., Deby, F. Corrosion and its Consequences for Reinforced Concrete Structures. ISTE Press – Elsevier. London, 2018. 232 p. doi.org/10.1016/C2016-0-01228-7
2. Lushnikova, V.Y., Tamrazyan, A.G. The effect of reinforcement corrosion on the adhesion between reinforcement and concrete. Magazine of Civil Engineering. 2018. No. 80(4). Pp. 128–137. DOI: 10.18720/MCE.80.12
3. Uglyanitsa, A.V., Gilyazidinova, N.V., Zhikharev, A.A., Kargin, A.A. Study of reinforcement corrosion in expanded clay concrete. HBRC Journal. 2015. 11(3). Pp. 307–310. doi.org/10.1016/j.hbrj.2014.08.001
4. Bonivento Bruges, J.C., Vieira, G., Revelo Orellana, D.P., Togo, I. Parameter of thermal resistance of bamboo multilayer wall. Magazine of Civil Engineering. 2018. 83(7). Pp. 92–101. DOI: 10.18720/MCE.83.9
5. Weerheijm, J. Understanding the tensile properties of concrete. A volume in Woodhead Publishing Series in Civil and Structural Engineering. Woodhead Publishing. Cambridge, 2013. 398 p.
6. Yildizel SA, Calis G. Design and optimization of basalt fiber added lightweight pumice concrete using taguchi method. Romanian Journal of Materials 2019. 49 (4). Pp. 544–553.
7. Choi, J., Lee B. Bonding properties of basalt fiber and strength reduction according to fiber orientation. Materials. 2015. 8. Pp. 6719–6727. doi.org/10.3390/ma8105335
8. Girgin, Z.C., Yildirim, M.T. Usability of basalt fibers in fiber reinforced cement composites. Materials and Structures. 2016. 49. Pp. 3309–3319. doi.org/10.1617/s11527-015-0721-4
9. Klyuev, S.V., Klyuev, A.V., Vatin, N.I. Fiber concrete for the construction industry. Magazine of Civil Engineering. 2018. 84(8). Pp. 41–47. DOI: 10.18720/MCE.84.4
10. Rassokhin, A.S., Ponomarev, A.N., Figovsky, O.L. The formation of the seabed surface relief near the gravitational object. Magazine of Civil Engineering. 2018. No. 79(3). Pp. 132–139. DOI: 10.18720/MCE.79.14
11. Ronaldo, E., Nerilli, F., Vairo, G. Basalt-based fiber-reinforced materials and structural applications in civil engineering. Composite Structures. 2019. 214. Pp. 246–263. doi.org/10.1016/j.compstruct.2019.02.002
12. Seydibeyoglu, M.O., Mohanty, A.K., Misra, M. Fiber technology for fiber-reinforced composites. A volume in Woodhead Publishing Series in Composites Science and Engineering. Woodhead Publishing. Cambridge, 2017. 336 p. doi.org/10.1016/C2015-0-05497-1
13. Rybakov, V.A., Ananeva, I.A., Pichugin, E.D., Garifullin, M. Heat protective properties of enclosure structure from thin-wall profiles with foamed concrete. Magazine of Civil Engineering. 2020. 94(2). Pp. 11–20. DOI: 10.18720/MCE.94.2
14. Figueiro, R. Fibrous and composite materials for civil engineering applications. Woodhead Publishing Series in Textiles. Woodhead Publishing. Cambridge, 2011. 420 p.
15. Jian-Jun, L., Ying, M., Yan-Chun, L. The performance of green basalt fiber and its application in the civil engineering field. Applied Mechanics and Materials. 2012. 193–194. Pp. 548–552. doi.org/10.4028/www.scientific.net/AMM.193-194.548

16. Gravit, M.V., Golub, E.V., Antonov, S.P. Fire protective dry plaster composition for structures in hydrocarbon fire. *Magazine of Civil Engineering*. 2018. No. 79(3). Pp. 86–94. DOI: 10.18720/MCE.79.9
17. Abed, F., Alhafiz, A.R. Effect of basalt fibers on the flexural behavior of concrete beams reinforced with BFRP bars. *Composite Structures*. 2019. 215. Pp. 23–34. doi.org/10.1016/j.compstruct.2019.02.050
18. Alnahhal, W., Aljidda, O. Flexural behavior of basalt fiber reinforced concrete beams with recycled concrete coarse aggregates. *Construction and Building Materials*. 2018. 169. Pp. 165–178. doi.org/10.1016/j.conbuildmat.2018.02.135
19. Duic, J., Kenno, S., Das, S. Performance of concrete beams reinforced with basalt fibre composite rebar. *Construction and Building Materials*. 2018. 176. Pp. 470–481. doi.org/10.1016/j.conbuildmat.2018.04.208
20. Jumaa, G.B., Yousif, A.R. Size effect on the shear failure of high-strength concrete beams reinforced with basalt FRP bars and stirrups. *Construction and Building Materials*. 2019. 209. Pp. 77–94. doi.org/10.1016/j.conbuildmat.2019.03.076
21. Jiang, C., Fan, K., Wu, F., Chen, D. Experimental study on the mechanical properties and microstructure of chopped basalt fiber reinforced concrete. *Materials and Design*. 2014. 58. Pp. 187–193. doi.org/10.1016/j.matdes.2014.01.056
22. Lago, B.D., Taylor, S.E., Deegan, P., Ferrara, L., Sonebi, M., Crosset, P., Pattarini, A. Full-scale testing and numerical analysis of a precast fibre reinforced self-compacting concrete slab pre-stressed with basalt fibre reinforced polymer bars. *Composites Part B: Engineering*. 2017. 128. Pp. 120–133. doi.org/10.1016/j.compositesb.2017.07.004
23. Lu, Z.Y., Xian, G.J., Li, H. Effects of exposure to elevated temperatures and subsequent immersion in water or alkaline solution on the mechanical properties of pultruded BFRP plates. *Composites Part B: Engineering*. 2015. 77. Pp. 421–430. doi.org/10.1016/j.compositesb.2015.03.066
24. Zhu, H., Cheng, S., Gao, D., Neaz, S.M., Li C. Flexural behavior of partially fiber-reinforced high-strength concrete beams reinforced with FRP bars. *Construction and Building Materials*. 2018. 161. Pp. 587–597. doi.org/10.1016/j.conbuildmat.2017.12.003
25. Karaburc, S.N., Yildizel, S.A., Calis, G.C. Evaluation of the basalt fiber reinforced pumice lightweight concrete. *Magazine of Civil Engineering*. 2020. 94(2). Pp. 81–92. DOI: 10.18720/MCE.94.7
26. Nepomuceno, M., Pereira-de-Oliveira, L.A., Pereira, S.F. Mix design of structural lightweight self-compacting concrete incorporating coarse lightweight expanded clay aggregates. *Construction and Building Materials*. 2018. 166. Pp. 373–385. doi.org/10.1016/j.conbuildmat.2018.01.161
27. Ahmad, M.R., Chen, B., Shah S.F. Investigate the influence of expanded clay aggregate and silica fume on the properties of lightweight concrete. *Construction and Building Materials*. 2019. 220. Pp. 253–266. doi.org/10.1016/j.conbuildmat.2019.05.171
28. Bodnarova, L., Hela, R., Hubertova, M., Novakova, I. Behaviour of lightweight expanded clay aggregate concrete exposed to high temperatures. *International Scholarly and Scientific Research & Innovation*. 2014. 8(12). Pp. 1210–1213.
29. Bogas, J.A., Gomes, M.G. and Real, S. Bonding of steel reinforcement in structural expanded clay lightweight aggregate concrete: The influence of failure mechanism and concrete composition. *Construction and Building Materials*. 2014. 65. Pp. 350–359. doi.org/10.1016/j.conbuildmat.2014.04.122
30. Hubertova, M. and Hela, R. Durability of lightweight expanded clay aggregate concrete. *Procedia Engineering*. 2013. 65. Pp. 2–6. doi.org/10.1016/j.proeng.2013.09.002
31. Lucas, S.S. Moxham, C., Tziviloglou, E., Jonkers, H. Study of self-healing properties in concrete with bacteria encapsulated in expanded clay. *Science and Technology of Materials*. 2018. 30(1). Pp. 93–98. doi.org/10.1016/j.stmat.2018.11.006
32. Pioro, L.S., Pioro, I.L. Production of expanded-clay aggregate for lightweight concrete from non-selfbloating clays. *Cement & Concrete Composites*. 2004. 26. Pp. 639–643. doi.org/10.1016/S0958-9465(03)00103-3
33. Yang, Y., Chen, B. Potential use of soil in lightweight foamed concrete. *Journal of Civil Engineering*. 2016. 20(6). Pp. 2420–2427. doi.org/10.1007/s12205-016-0140-2
34. Koyankin, A.A., Mitasov, V.M., Tskhay, T.A. Compatibility of precast heavy and monolithic lightweight concretes deforming. *Magazine of Civil Engineering*. 2018. 84(8). Pp. 162–172. DOI: 10.18720/MCE.84.16
35. Sergeev, V.V., Petrichenko, M.R., Nemova, D.V., Kotov, E.V., Tarasova, D.S., Nefedova, A.V., Borodinecs, A.B. The building extension with energy efficiency light-weight building walls. *Magazine of Civil Engineering*. 2018. 84(8). Pp. 67–74. DOI: 10.18720/MCE.84.7
36. Borovskikh, I.V., Morozov, N.M. Increased durability of basalt fiber in cement concrete. *Building materials and products*. *Izvestia KGASU* 2012. 2(20). Pp. 160–165.
37. Singh, S.K., Kirthika, S., Maruthupandian, S. Durability Studies on Basalt Fibre Reinforced Concrete. *Indian Concrete Journal*. 2018. 92(4). Pp. 45–55.
38. Thompson, M.K. and Thompson, J.M. *ANSYS mechanical APDL for finite element analysis*. Butterworth-Heinemann. Oxford, 2017. 466 p.
39. Lam, T.V., Vu, D.T., Dien, V.K., Bulgakov, B.I., Korol, E.A. Properties and thermal insulation performance of lightweight concrete. *Magazine of Civil Engineering*. 2018. 84(8). Pp. 173–191. DOI: 10.18720/MCE.84.17
40. Rao, S.S. *The finite element method in engineering*. Butterworth-Heinemann. Oxford, 2018. 782 p. doi.org/10.1016/C2016-0-01493-6
41. Stolarski, T., Yoshimoto, S., Nakasone, Y. *Engineering analysis with ANSYS software*. Butterworth-Heinemann. Oxford, 2018. 562 p. doi.org/10.1016/C2016-0-01966-6
42. GOST 10180-2012. *Concretes. Methods for strength determination using reference specimens*. Moscow, 2013. 30 p.
43. ACI 211.1-91: *Standard practice for selecting proportions for normal, heavyweight, and mass concrete (Reapproved 2009)*. ACI Committee 211, 2002. 38 p.

### **Contacts:**

*Vera Galishnikova, galishnikova-vv@rudn.ru*

*Makhmud Kharun, miharun@yandex.ru*

*Dmitry Dmitrievich Koroteev, koroteev-dd@rudn.ru*

*Paschal Chimerezeze Chiadighikaobi, passyding2@mail.ru*